Melatonin regulation of transcription in the reversal of morphine tolerance: Microarray analysis of differential gene expression

YU-CHE CHENG[1-3*], RU-YIN TSAI[4*], YEN-TSENG SUNG[1], ING-JUNG CHEN[5], TZU-YI TU[1], YA-YUAN MAO[1] and CHIH-SHUNG WONG[2,5,6]

[1]Proteomics Laboratory, Department of Medical Research, Cathay General Hospital, Taipei 10630; [2]School of Medicine, Fu Jen Catholic University, New Taipei City 24205; [3]Department of Biomedical Sciences and Engineering, National Central University, Jhongli 32001; [4]College of Nursing and Health Sciences, Da-Yeh University, Changhua 51591; [5]Department of Anesthesiology, Cathay General Hospital, Taipei 10630; [6]Institute of Medical Science, National Defense Medical Center, Taipei 11490, Taiwan, R.O.C.

Received June 20, 2018; Accepted December 11, 2018

DOI: 10.3892/ijmm.2018.4030

Abstract. Tolerance and associated hyperalgesia induced by long-term morphine administration substantially restrict the clinical use of morphine in pain treatment. Melatonin, a neurohormone released by the pineal gland, has been demonstrated to attenuate anti-nociceptive morphine tolerance. The present study investigates differentially expressed genes in the process of morphine tolerance and altered gene expression subsequent to melatonin treatment in chronic morphine-infused ratspinal cords. Morphine tolerance was induced in male Wistar rats by intrathecal morphine infusion (the MO group). Melatonin (the MOMa group) was administered to overcome the effects derived by morphine. The mRNA collected from L5-S3 of the spinal cord was extracted and analysed by rat expression microarray. Principal component analysis and clustering analysis revealed that the overall gene profiles were different in morphine and melatonin treatments. Subsequent to Gene Ontology analysis, the biological processes of differentially expressed genes of MO and MOMa compared with the control group were constructed. Furthermore, a panel of genes exclusively expressed following melatonin treatment and another panel of genes with inverse expression between the MO and MOMa group were also established. Subsequent to PANTHER pathway analysis, a group of genes with inverse expression following melatonin administrated compared with morphine alone were identified. The expression levels of genes of interest were also confirmed using a reverse transcription-quantitative polymerase chain reaction. The gene panel that was constructed suggests a potential signaling pathway in morphine tolerance development and is valuable for investigating the mechanism of morphine tolerance and the regulatory gene profiles of melatonin treatment. These results may contribute to the discovery of potential drug targets in morphine tolerance treatments in the future.

Correspondence to: Dr Chih-Shung Wong, Department of Anesthesiology, Cathay General Hospital, 280 Renai Road, Taipei 10630, Taiwan, R.O.C.
E-mail: w82556@gmail.com

*Contributed equally

Key words: melatonin, morphine tolerance, gene expression

Introduction

Morphine is a powerful analgesic agent used for treating acute and chronic pain in surgical interventions or in hospice care (1). However, long-term administration of morphine induces tolerance and hyperalgesia. Furthermore, adverse effects, including addiction, dependence, constipation and respiratory depression limit its clinical usefulness (2,3). The physiological responses of morphine tolerance include opioid receptor uncoupling, endocytosis/desensitization (4), increased binding of β-arrestin to opioid receptors, glutamatergic receptor activation and neuroinflammation (5). Melatonin is a neurohormone derived from serotonin and is released from the pineal gland (6). It is used for sleep modulation and relieves the stress caused by sleep disturbance (1). It has previously been revealed that melatonin treatment partially reverses morphine tolerance by inhibiting microglia activation though a heat shock protein 27 (HSP27)-associated pathway (7). Furthermore, melatonin co-treatment was revealed to prevent morphine-induced hyperalgesia and tolerance in rats, potentially by inhibiting protein kinase C-associated pathways (8,9). A report also demonstrated that decreased mitochondrial DNA copy numbers in the hippocampus during opiate addiction were mediated by autophagy and may be reversed by melatonin (10). Additionally, melatonin was revealed to enhance the reward behaviour of morphine via the nitric oxidergic pathway (11). Raghavendra and Kulkarni initially reported that the systemic administration of melatonin reversed morphine-induced tolerance in mice (12). Song *et al* (8) identified that daily intraperitoneal melatonin treatment reduced morphine tolerance in rats via the regulation of the N-methyl-D-aspartate receptor

subunit 1. Furthermore, Garmabi *et al* (13) observed a reduction of melatonin levels in rats under constant light exposure; those animals also presented a high morphine consumption and severe morphine withdrawal syndrome. Fan *et al* (14) further reported a substantial decrease of serum melatonin and melatonin receptor 1 mRNA subsequent to chronic morphine infusion in rats. Previously, not only was it revealed that melatonin treatment partially reversed morphine tolerance by inhibiting microglia activation though a HSP27-associated pathway (7), but preliminary examinations additionally revealed that chronic morphine treatment resulted in transcriptomics changes. All studies noted that melatonin participates in the morphine tolerance pathway. Although melatonin was demonstrated to diminish morphine tolerance, the transcriptomic changes derived from melatonin treatment in opiate tolerance remain undetermined. To search whole genome expression profiles disturbed by long-term morphine administration and clarify the gene alterations caused by melatonin, an expression array was used in the present study to examine the effects of melatonin treatment on morphine-induced tolerance in rats. The results may provide insight on and contribute to deciphering the detailed mechanisms of morphine tolerance.

Materials and methods

Construction of intrathecal catheters. The intrathecal (i.t.) catheters were constructed by inserting a 3.5 cm Silastic tube (Corning Incorporated, Corning, NY, USA) into an 8 cm polyethylene tube (0.008 inch internal diameter, 0.014 inch outer diameter; Spectranetics, Colorado Springs, CO, USA) and sealing the joint with epoxy resin and silicon rubber as previously described (15).

Animal preparation and intrathecal drug delivery. The use of rats in the present study adhered to the Guiding Principles in the Care and Use of Animals of the American Physiology Society (16) and was ethically approved by the National Defense Medical Center Animal Care and Use Committee (Taipei, Taiwan). A total of 27 Male Wistar rats (350-400 g), each rat (with 12 weeks of age) was housed individually at a room temperature at 25˚C, at 1 atm, with water and food freely as wish. The rats were anaesthetized with phenobarbital (65 mg/kg, intraperitoneally) and two i.t. catheters were implanted. The catheters were inserted via the atlantooccipital membrane down to spinal cord segments L5, L6 and S1-S3, which are associated with the tail-flick reflex (17). One catheter was connected to a mini-osmotic pump (Alzet, Cupertino, CA, USA) for an infusion of saline or morphine (15 μg/h) for 7 days at a rate of 1 μl/h. Subsequent to catheterization (day 0), the rats were returned to their home cages and maintained in a 12 h light/dark cycle with *ad libitum* access to food and water. Rats with neurological deficits were excluded. On day 7, by which time a morphine tolerance had developed, the catheter used for saline or morphine infusion was cut and blocked with a metal metal plug to prevent CSF leakage. The rats were injected i.t. via the second catheter with 5 μl either with vehicle (10% ethanol) or melatonin (50 μg in 10% ethanol), then, 30 min later, a single dose of morphine (15 μg in 5 μl saline, i.t.) was injected and the antinociceptive

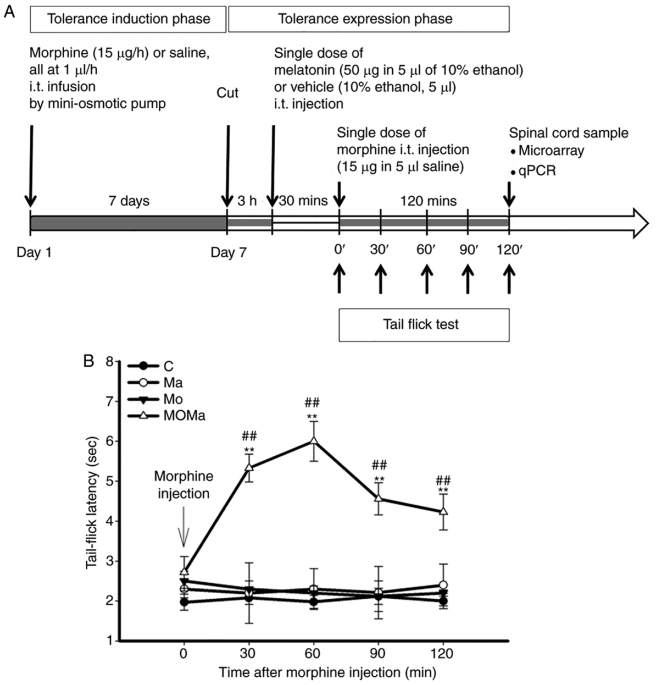

Figure 1. Experimental procedure and effect of melatonin on the antinociceptive effect in morphine-tolerant rats. (A) Experimental procedure for drug administration. Male Wistar rats were implanted with two i.t. catheters, one of which was connected to a mini-osmotic pump for the infusion of morphine or saline for 7 days. On day 7, subsequent to morphine tolerance development, the catheter was cut, and 3 h later the rats were injected intrathecally with either vehicle or melatonin via the second catheter. A total of 30 min later, a single dose of morphine (15 μg) was injected intrathecally and its antinociceptive effect measured. (B) Melatonin reverses the antinociceptive effect of morphine in morphine-tolerant rats. Antinociception of morphine was assessed on day 7 following intrathecal infusion of saline or morphine. At 3 h subsequent to the discontinuation of infusion, the rats were injected intrathecally with 10% ethanol (as vehicle) or 50 μg melatonin. After 30 min, the rats underwent a 15 μg morphine administration, then tail-flick latency was measured every 30 min for 120 min. All data are presented as the mean ± standard error of the mean for at least 5 rats. **P<0.01 vs. the Ma group; $^{\#\#}$P<0.01 vs. the MO group. C, control (saline infusion/vehicle injection/saline challenge); MO, morphine (morphine infusion/vehicle injection/morphine challenge); Ma, melatonin (morphine infusion/melatonin injection/saline challenge); MOMa, (morphine infusion/melatonin injection/morphine challenge); i.t., intrathecal; qPCR, quantitative polymerase chain reaction.

effect measured. The protocol is presented in Fig. 1A. There were four experimental groups used in the present study, as follows: Controls, melatonin-treated, morphine-treated and those treated with melatonin and morphine combined. For the control group, the animals were infused with saline for 7 days and infused with vehicle injection for 30 min, and subsequently injected with saline. For the morphine group, the animals were infused with morphine for 7 days, injected with vehicle injection for 30 min and subsequently injected with morphine. For the melatonin group, the animals were infused with morphine for 7 days and injected with melatonin for 30 min, and subsequently injected with saline. For the melatonin and morphine group, the animals were infused with morphine for 7 days, injected with melatonin for 30 min and subsequently injected with morphine.

The dose of morphine selected was based on a previous study (18). For i.t. injection, melatonin was dissolved in ethanol (50 μg/5 μl in 10% ethanol maximum). All drugs were

purchased from Sigma-Aldrich (Merck KGaA, Darmstadt, Germany) and were delivered i.t., followed by the flushing of the catheter with 5 μl saline. Preliminary results revealed no abnormal motor function subsequent to i.t. injection of the test drugs (data not shown).

Antinociception test. Tail-flick latency was measured using the hot water immersion test (52±0.5˚C). Baseline latency was ~2±0.38 sec, and a cutoff time of 10 sec was used. Rats were placed in plastic restrainers for drug injection and antinociception testing.

Spinal cord sample collection from rats with different treatments. Spinal cord sample collection was performed as previously described (7), and morphine tolerance in rats was confirmed by the time-course of tail-flick latency over a 7-day period. Prior to day 4, the rats with morphine infusions demonstrated a reduction of tail-flick latency compared with the saline-infused group, which exhibited no changes in latency during the period. Substantial morphine tolerance was developed on day 7 as determined by a significant reduction of the antinociceptive effect of morphine compared with day one, with a reduction of the tail-flick latency of ~60%. And then, rats were i.t. injected with either 10% ethanol (as a vehicle) or melatonin via the externalized i.t. catheter. A total of 30 min later, a single dose of morphine (15 μg) was injected i.t. to confirm morphine tolerance. In contrast, melatonin pretreatment attenuated morphine tolerance, melatonin pretreatment was done by administering melatonin on day 7, at 30 min prior to morphine intrathecal injection. The lumbar enlargement segment was removed from 4 rat spinal cords from each group for differential gene expression analysis.

Spinal cord sample preparation. Following drug treatment, the rats were sacrificed by exsanguination under anaesthesia with isoflurane (Abbott Pharmaceutical Co. Ltd., Lake Bluff, IL, USA) and a laminectomy was performed at the lower edge of the 12th thoracic vertebra. Subsequently, the lumber enlargement (L5-S3) of the spinal cord was immediately collected for subsequent analysis.

Rat expression microarray. Following the tail-flick test, the rats were sacrificed, and lumber enlargement (L5-S3) of the spinal cord was immediately collected. There were 4 samples tested in each group. Total mRNAs were extracted using TRIzol reagent (Invitrogen; Thermo Fisher Scientific, Inc., Waltham, MA, USA). RNA concentration and purity were assessed using an Agilent 2100 Bioanalyzer (Agilent Technologies, Inc., Santa Clara, CA, USA) with a criteria of OD260/OD280 (>1.8) and OD260/OD230 (>1.6). Next, the RNAs were labelled with Cy5 dye by an indirect NHS ester labelling kit (GE Healthcare, Chicago, IL, USA) according to the manufacturer's protocol. The labelled RNAs were hybridized with a Rat OneArray® microarray (Phalanx Biotech Group, Hsinchu, Taiwan), which contains 24,358 rat genome probes and 980 experimental control probes. All the probes correspond to annotated genes in RefSeq and Ensembl databases. The hybridization procedure was performed at 50˚C in a Phalanx Hybridization System (Phalanx Biotech Group). A total of 16 h after hybridization, non-specific binding targets were washed away using three sequential washing steps by 2X saline-sodium citrate buffer (SSC) contained 0.2% SDS solution for 5 min at 42˚C. Then, the slide was spun dry with a centrifuge for 1 min at room temperature. The images of the microarray were scanned using an Agilent G2505C scanner (Agilent Technologies, Inc.). The Cy5 fluorescence intensities of each spot were analysed by GenePix 4.1 software (Molecular Devices, LLC, Sunnyvale, CA, USA).

Microarray analysis. Microarray spot analysis was resolved by the Rosetta Resolver System® (Rosetta Biosoftware, Seattle, WA, USA). Control probes data were calculated, and the reproducibility of each microarray slide was assessed using Pearson's correlation coefficient calculations with a criterion of R-value >0.975. Normalized spot intensities were transformed to gene expression $\log_2$ ratios in each group. For further analysis, the spots with a $\log_2$ ratio ≥1 or a $\log_2$ ratio ≤-1 or undetectable $\log_2$ ratios but with differences in intensity between the two samples of >1,000 and a $P<0.05$ were selected according to the method of Pirooznia *et al* (19). Principal Component Analysis (PCA) was performed to evaluate any differences among biological replicates and their treatment conditions using FDA released ArrayTrack™ HCA-PCA Standalone Package (20). PCA uses an orthogonal transformation to convert a set of observations of possibly correlated variables into a set of values of uncorrelated variables called principal components. For advanced data analysis, intensity data were pooled and calculated to identify differentially expressed genes based on the threshold of fold-change and P-value. The correlation of expression profiles between samples and treatment conditions was demonstrated by unsupervised hierarchical clustering analysis. Average linkage clustering was performed to visualize the correlations among the replicates and varying sample conditions using and open source software, Java Treeview (21). Up and downregulated genes are represented in red and green colors, respectively.

Gene ontology (GO) enrichment analysis. The gene IDs of interest were uploaded to the Gene ontology Enrichment analysis website (22). The database and analysis services were funded by the National Human Genome Research Institute in the U.S. And right now the website were maintained and updated by the Gene Ontology Consortium (GOC). The names of the genes with interested were paste to the query column in the website and set the GO aspect as molecular function for the analysis. The database search was confined to *Rattus norvegicus* database.

Gene pathway mapping by PANTHER. The gene IDs of interest were uploaded to the PANTHER Classification System website (http://pantherdb.org). PANTHER is a comprehensive, curated database of protein families, trees, subfamilies, functions and ontology (23). The search parameter was set to 'molecular function', and the database search was confined to only the *Rattus norvegicus* database. The keywords used were the gene names of interest and the access date were December 12 and 19, 2017.

Table I. Primers used for reverse transcription-quantitative polymerase chain reaction analysis.

Target gene	Gene ID	Position	Sequence
G protein subunit β 1 (Gnb1)	NM_030987.2	F:262-281 R:317-337	5'-tccagtgggaagaatccaaa-3' 5'-ccagtgcatggcataaatctt-3'
Cholecystokinin B receptor (Cckbr)	NM_013165.2	F:1799-1819 R:1842-1861	5'-cccgtttgacttcattattgc-3' 5'-tgaaaggcgtgtggttgata-3'
5-hydroxytryptamine receptor 1A (Htr1a)	NM_012585.1	F:1054-1072 R:1110-1128	5'-ggcaccttcatcctctgct-3' 5'-gtggcagctgctttcacag-3'
RAS protein activator like 1 (Rasal1)	NM_001108335.1	F:408-429 R:451-470	5'-ggagtacactgttcaccttcca-3' 5'-tcctcatccagcacgtagaa-3'
General transcription factor 2A subunit 1 like (Gtf2a1l)	NM_001012136.1	F:1222-1242 R:1267-1289	5'-gaggatcccctaaattctgga-3' 5'-ttatctgtgtcaaacaggtctgg-3'
Period circadian clock 1 (Per1)	NM_001034125.1	F:1986-2008 R:2043-2062	5'-tcctaacacaaccaagcgtaaat-3' 5'-ccctctgcttgtcatcatca-3'
Methionine adenosyltransferase 2A (Mat2a)	NM_134351.1	F:149-168 R:204-222	5'-tgtaggggaaggtcatccag-3' 5'-cctgctgaaggtgtgcatc-3'
Collagen type V α 3 chain (Col5a3)	NM_021760.1	F:634-652 R:673-693	5'-cggggaggagtcttttgag-3' 5'-gcctgagggtctggaattaac-3'
Inositol 1,4,5-trisphosphate receptor, type 3 (Itpr3)	NM_013138.1	F:8362-8381 R:8403-8422	5'-taggggatgcaagttctcca-3' 5'-ccactgagaaatgccagtca-3'
Diacylglycerol kinase ζ (Dgkz)	NM_031143.1	F:330-347 R:410-429	5'-ctttgggcacaggaaagc-3' 5'-gatctgccgctcagattcac-3'
LIM zinc finger domain containing 2 (Lims2)	NM_001012163.1	F:966-985 R:1032-1051	5'-tcatgtgattgagggtgacg-3' 5'ccaccaggagaacagactgg-3'

F, forward; R, reverse.

RNA extraction and reverse transcription-quantitative polymerase chain reaction (RT-qPCR). Tissues were collected as described above. RNA was extracted within 1 h at room temperature using TRIzol reagent following manufacturer's protocol (Invitrogen; Thermo Fisher Scientific, Inc.). mRNA were reverse transcribed to cDNA using the SuperScript III First-Strand Synthesis System (Invitrogen; Thermo Fisher Scientific, Inc.). cDNA were amplified and subjected to optical analysis to verify the integrity of extracted RNA. The expression of target genes were quantified for all experimental groups using LightCycler system (Roche Diagnostics, Basel, Switzerland). RT-qPCR analysis thermocycling conditions were: 95˚C for 10 min and then the cycling conditions were set as 95˚C for 10 sec, 60˚C for 20 sec, 72˚C for 40 sec for 50 cycles. The method of quantification for RT-qPCR products were followed Livak and Schmittgen *et al* (24) The relative abundance of transcripts were normalized to the constitutive expression of GAPDH. The primers of each genes used in RT-qPCR were listed in Table I.

Data and statistical analyses. All data are presented as the mean ± standard error of the mean. Statistical analysis was performed using SigmaStat 3.0 software (SYSTAT Software Inc., San Jose, CA, USA). Tail-flick latencies were analyzed using two-way (time and treatment) analysis of variance (ANOVA), followed by one-way ANOVA with a *post hoc* Student-Newman-Keuls test. The RT-qPCR results were analyzed using a Student's t-test. $P<0.05$ was considered to indicate a statistically significant difference.

Results

Experimental design and procedure. The experimental procedure for drug administration was depicted in Fig. 1. Male Wistar rats were implanted with two i.t. catheters and connected to a mini-osmotic pump for morphine or saline infusion for 7 days for morphine tolerance induction. On day 7, subsequent to the development of tolerance, the catheter was cut, and 3 h later, the rats received an i.t. injection of either vehicle or melatonin via the other catheter. A total of 30 min later, at the tolerance expression phase, a single dose of morphine (15 μg) was injected i.t., and the antinociceptive effect was measured. Tail flick tests were performed in every experimental group and the results were presented in Fig. 1B. There was a significant reduction of morphine tolerance subsequent to melatonin addition compared with the control group ($P<0.01$). Following a tail-flick test, the rats were sacrificed, and the L5 to S3 region of the spinal cords were collected for further analysis.

Differential gene expression among morphine tolerance, melatonin treatment and morphine tolerance combined with melatonin treatment groups. To determine the alterations in gene expression caused by morphine and reversed by melatonin treatment in rat spinal cords, rat global gene expression profiles of four independent RNA samples from each group

Table II. Number of differentially expressed genes.

Group comparison	Upregulated	Downregulated
MO/C	162	16
MOMa/C	290	15
Ma/C	476	71

Standard selection criteria to identify differentially expressed genes are as follows: i) $\log_2$ |Fold changel≥1 and P<0.05; ii) $\log_2$ ratios='NA' and the differences of intensity between the two samples ≥1000. Detail gene lists were be provided by request. C, control (saline infusion/vehicle injection/saline challenge); Mo, morphine (morphine infusion/vehicle injection/morphine challenge); Ma, melatonin (morphine infusion/melatonin injection/saline challenge); MOMa, (morphine infusion/melatonin injection/morphine challenge).

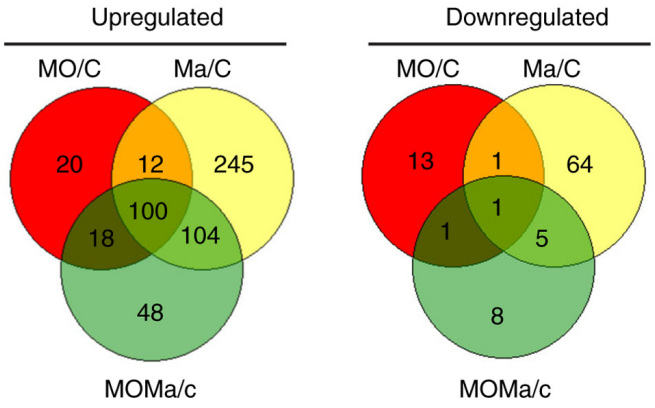

Figure 2. Venn diagram analysis of the genes that were upregulated (left) or downregulated (right) by morphine tolerance and/or melatonin treatment compared with the control group. In each pair test, the upregulated genes were identified as follows: Log_2 |Fold changel ≥ 1 and P<0.05 In the diagram, red circles represent genes putatively affected by long-term morphine application, yellow circles represent genes influenced by melatonin treatment and green circles represent genes for which melatonin-induced expression changes were putatively affected by morphine. All genes considered were differentially expressed compared with the untreated group. C, control (saline infusion/vehicle injection/saline challenge); MO, morphine (morphine infusion/vehicle injection/morphine challenge); Ma, melatonin (morphine infusion/melatonin injection/saline challenge); MOMa, (morphine infusion/ melatonin injection/morphine challenge).

were selected for microarray analysis. PCA and clustering analysis revealed that the overall gene profiles derived from microarray analysis were separated based on morphine or melatonin treatment. The result revealed that 162 genes were upregulated and 16 genes were downregulated in the morphine-tolerant group (MO group, n=7) compared with the control group (C group, n=5); 476 genes were upregulated and 71 genes were downregulated in the melatonin treatment group (Ma group, n=5) compared with the control group (C group), and 290 genes were upregulated and 15 genes were downregulated in the morphine with acute melatonin treatment group (MOMa group, n=10) compared with the control group (Table II). All genes selected using the criteria of $\log_2$|Fold changel≥ 1 and P<0.05 or undetectable $\log_2$ ratios but with differences in intensity between the two samples of >1,000. Statistical significance was used to avoid confounding due to variation amongst the animals and addressed additional evidence that the transcriptional profiles of morphine tolerance and melatonin treatment *in vivo* are different. The present study compared the number of upregulated genes between the MO and MOMa groups; it was identified that the number of upregulated genes in the MOMa group was greater compared with the number in the MO group, which indicated that melatonin restored the antinociceptive effect of morphine, which was accomplished with multiple gene expression alterations.

Gene ontology (GO) analysis of the altered genes from the MO or MOMa group. The differentially expressed genes were then subjected to GO analysis based on molecular function (Table III). Numerous GO terms were identical between the two groups; however, opsonin binding, actin binding, calcium ion binding, sugar binding, oxidase activity, deaminase activity, protein complex binding and oxidoreductase activity were not identified in the MO group. On the other hand, GTPase activity, phospholipase inhibitor activity, cytokine activity, GTP binding, guanyl-nucleotide and ribonucleotide binding, immunoglobulin (Ig)G receptor activity, IgE binding and protein dimerization activity were not identified in the MOMa group, implying the potential regulatory mechanism of melatonin treatment. From the GO terms identified between the MO and MOMa groups, it was revealed that a number of notable pathways were altered. It has been previously reported that the morphine tolerance process involves inflammation (25). Immune-associated processes, including cytokine activity, IgG receptor activity and IgE binding, were missing following melatonin treatment, which indicates that melatonin treatment may participate in the downregulation of these cellular process. On the other hand, the gene expression for actin binding was present following melatonin treatment; this result implies that cytoskeleton reconstitution may be activated. Additionally, genes involving calcium ion binding, sugar binding, NADPH oxidase activity, deaminase activity and protein complex binding pathways appeared subsequent to melatonin treatment, indicating the requirement for the metabolic activity that emerged following melatonin treatment. The gene expression data for IgG receptor expression and actin binding were selected and provided by request.

Venn diagram and genes exclusively expressed in the MOMa group. In order to clarify the differential gene expression panels among the three groups, Venn diagram analysis was performed, and the results depicted the overlap of differentially expressed genes between the MO, Ma and MOMa groups (Fig. 2). In total, 48 genes were upregulated and 8 were genes downregulated exclusively in the MOMa group. These genes were the candidates that participated in the reversal of morphine tolerance. It was also identified that 20 genes were upregulated and 13 genes were downregulated exclusively in the MO group; these genes were not altered by melatonin treatment, so these genes were not involved in the melatonin reversal effect in morphine tolerance. All the genes in Venn diagram analysis are listed in Table IV-A and -B. Genes expressed exclusively in the MOMa group are notable as they may be the targets for the reversal of morphine tolerance associated with melatonin in future studies. From Table IV-B, the myocilin gene demonstrated the greatest

Table III. Identified gene ontology terms of the MO and MOMa groups compared with the C group.

	MO/C			MOMa/C		
Geneset name	No. of genes in geneset	No. of genes in overlap	P-value	No. of genes in geneset	No. of genes in overlap	P-value
GO:0001846-opsonin binding		N.I.		7	3	<0.01
GO:0001871-pattern binding	116	7	<0.01	116	13	<0.01
GO:0001872-zymosan binding	3	2	0.02	3	2	0.04
GO:0003924-GTPase activity	98	4	0.05		N.I.	
GO:0003779-actin binding		N.I.		233	10	0.01
GO:0004857-enzyme inhibitor activity	238	10	<0.01	238	11	<0.01
GO:0004859-phospholipase inhibitor activity	6	2	0.05		N.I.	
GO:0004866-endopeptidase inhibitor activity	148	6	0.01	148	7	0.02
GO:0005125-cytokine activity	110	5	0.01		N.I.	
GO:0005506-iron ion binding	289	7	0.03	289	10	0.03
GO:0005525-GTP binding	312	8	0.02		N.I.	
GO:0005509-calcium ion binding		N.I.		672	20	0.01
GO:0005529-sugar binding		N.I.		215	9	0.02
GO:0005539-glycosaminoglycan binding	102	5	0.01	102	11	<0.01
GO:0008009-chemokine activity	32	5	<0.01	32	4	0.01
GO:0008201-heparin binding	72	4	0.02	72	8	<0.01
GO:0016175-superoxide-generating NADPH oxidase activity		N.I.		7	3	<0.01
GO:0016814~hydrolase activity, acting on carbon-nitrogen (but not peptide) bonds, in cyclic amidines	22	3	0.01	22	4	<0.01
GO:0019239-deaminase activity		N.I.		21	3	0.04
GO:0019001-guanyl nucleotide binding	326	8	0.02		N.I.	
GO:0019763-immunoglobulin receptor activity	7	3	<0.01	7	3	<0.01
GO:0019770-IgG receptor activity	4	2	0.03		N.I.	
GO:0019834-phospholipase A2 inhibitor activity	3	2	0.02	3	2	0.04
GO:0019863-IgE binding	4	2	0.03		N.I.	
GO:0019864-IgG binding	6	4	<0.01	6	4	<0.01
GO:0019865-immunoglobulin binding	12	5	<0.01	12	5	<0.01
GO:0019955-cytokine binding	87	4	0.04	87	7	<0.01
GO:0020037-heme binding	148	5	0.04	148	7	0.02
GO:0030246-carbohydrate binding	337	10	<0.01	337	20	<0.01
GO:0030247-polysaccharide binding	116	7	<0.01	116	13	<0.01
GO:0030414-peptidase inhibitor activity	159	7	<0.01	159	8	0.01
GO:0032403-protein complex binding		N.I.		222	12	<0.01
GO:0032561-guanyl ribonucleotide binding	326	8	0.02		N.I.	
GO:0042379-chemokine receptor binding	33	5	<0.01	33	4	0.01
GO:0042802-identical protein binding	588	11	0.02	588	18	0.01
GO:0042803-protein homodimerization activity	318	8	0.02	318	15	<0.01
GO:0046906-tetrapyrrole binding	154	5	0.04	154	7	0.03
GO:0046983-protein dimerization activity	528	10	0.03	528	20	<0.01
GO:0048020-CCR chemokine receptor binding	3	2	0.02		N.I.	
GO:0050664-oxidoreductase activity, acting on NADH or NADPH, with oxygen as acceptor		N.I.		11	3	0.01

N.I., not identified; Ig, immunoglobulin; GO, Gene Ontology; C, control (saline infusion/vehicle injection/saline challenge); Mo, morphine (morphine infusion/vehicle injection/morphine challenge); Ma, melatonin (morphine infusion/melatonin injection/saline challenge); MOMa, (morphine infusion/melatonin injection/morphine challenge).

Table IV. Top 20 exclusively upregulated and downregulated genes in each group.

A, Exclusively expressed genes in MO group

Gene symbol	Description	Gene ID	Fold-change
Ddx60	DEAD (Asp-Glu-Ala-Asp) box polypeptide 60, probable ATP-dependent RNA helicase DDX60-like	100360801	1.61 Up
Lgals3bp	Lectin, galactoside-binding, soluble, 3 binding protein	245955	1.54 Up
Oas1a	2'-5' oligoadenylate synthetase 1A	192281	1.47 Up
Isg15	ISG15 ubiquitin-like modifier	298693	1.46 Up
Slamf9	SLAM family member 9	289235	1.29 Up
Usp18	Ubiquitin specific peptidase 18	312688	1.28 Up
Smim5	Small integral membrane protein 5	689926	1.26 Up
Casp4	Caspase 4, apoptosis-related cysteine peptidase	114555	1.2 Up
Cd33	CD33 molecule	690492	1.2 Up
Pik3ap1	Phosphoinositide-3-kinase adaptor protein 1	294048	1.14 Up
Ccl7	Chemokine (C-C motif) ligand 7	287561	1.13 Up
Apol9a	Apolipoprotein L 9a	503164	1.11 Up
Dpt	Dermatopontin	289178	1.09 Up
Cryaa	Crystallin, αA	24273	1.06 Up
Irgm	Immunity-related GTPase family, M	303090	1.05 Up
Irf7	Interferon regulatory factor 7	293624	1.04 Up
Gpr160	G protein-coupled receptor 160	499588	1.03 Up
Uba7	Ubiquitin-like modifier activating enzyme 7	301000	1.03 Up
Vwa5b1	Von Willebrand factor A domain containing 5B1	313653	1.03 Up
Olr104	Olfactory receptor 104	293243	1.02 Up
LOC689064	β-globin	689064	-1 Down
Fras1	Fraser syndrome 1	289486	-1.01 Down
Zfp597	Zinc finger protein 597	266774	-1.06 Down
LOC681849	Similar to protein C6orf142 homolog	681849	-1.09 Down
Alas2	Aminolevulinate, delta-, synthase 2	25748	-1.13 Down
LOC500300	Similar to hypothetical protein MGC6835	500300	-1.2 Down
Hspa1b	Heat shock 70 kD protein 1B (mapped)	294254	-1.21 Down
Ccdc77	Coiled-coil domain containing 77	312677	-1.3 Down
Oas1e	2'-5' oligoadenylate synthetase 1E	494201	-1.4 Down
Pmp2	Peripheral myelin protein 2	688790	-1.47 Down
Fkbp6	FK506 binding protein 6	288597	-1.98 Down
Prx	Periaxin	78960	-2.16 Down
Mpz	Myelin protein zero	24564	-2.92 Down

B, Exclusively expressed genes in MOMa group

Gene symbol	Description	Gene ID	Fold-change
Myoc	Myocilin	81523	2.47 Up
Samsn1	SAM domain, SH3 domain and nuclear localization signals, 1	170637	1.48 Up
Scin	Scinderin	298975	1.45 Up
Ncan	Neurocan	58982	1.35 Up
Tagln	Transgelin	25123	1.34 Up
Aplnr	Apelin receptor	83518	1.31 Up
Nlrc4	NLR family, CARD domain containing 4	298784	1.28 Up
S1pr3	Sphingosine-1-phosphate receptor 3	306792	1.27 Up
Mxra8	Matrix-remodelling associated 8	313770	1.26 Up
Sptbn5	Spectrin, β, non-erythrocytic 5	296090	1.24 Up

Table IV. Continued.

B, Exclusively expressed genes in MOMa group

Gene symbol	Description	Gene ID	Fold-change
Plin2	Perilipin 2	298199	1.23 Up
Epyc	Epiphycan	314772	1.23 Up
Chdh	Choline dehydrogenase	290551	1.22 Up
Hlx	H2.0-like homeobox	364069	1.19 Up
Cenpf	Centromere protein F	257649	1.19 Up
Aoah	Acyloxyacyl hydrolase (neutrophil)	498757	1.17 Up
Spta1	Spectrin, α, erythrocytic 1 (elliptocytosis 2)	289257	1.15 Up
Trim47	Tripartite motif-containing 47	690374	1.14 Up
Abi3	ABI family, member 3	303476	1.13 Up
Ssc5d	Scavenger receptor cysteine rich domain containing (5 domains)	308341	1.13 Up
Epm2aip1	EPM2A (laforin) interacting protein 1	316021	-1.02 Down
LOC691921	Hypothetical protein LOC691921	691921	-1.04 Down
Klhl11	Kelch-like 11 (*Drosophila*)	287706	-1.09 Down
Ppargc1b	Peroxisome proliferator-activated receptor γ, coactivator 1 β	291567	-1.11 Down
Pcdhb6	Protocadherin β6	291653	-1.14 Down
Tox2	TOX high mobility group box family member 2	311615	-1.22 Down
Map9	Microtubule-associated protein 9	310544	-1.26 Down
RGD1309108	Similar to hypothetical protein FLJ23554	315578	-1.55 Down

C, Exclusively expressed genes in Ma group

Gene symbol	Description	Gene ID	Fold-change
Defb3	β-defensin 3	641623	3.52 Up
RT1-Da	RT1 class II, locus Da	294269	2.60 Up
RT1-Ba	RT1 class II, locus Ba	309621	2.59 Up
Pxmp4	Peroxisomal membrane protein 4	282634	2.46 Up
RT1-Bb	RT1 class II, locus Bb	309622	2.21 Up
Ccl11	Chemokine (C-C motif) ligand 11	29397	2.08 Up
Tmem252	Transmembrane protein 252	361744	2.07 Up
Aurkb	Aurora kinase B	114592	1.99 Up
Cd74	Cd74 molecule, major histocompatibility complex, class II invariant chain	25599	1.89 Up
Birc5	Baculoviral IAP repeat-containing 5	64041	1.81 Up
Lmcd1	LIM and cysteine-rich domains 1	494021	1.80 Up
Fam111a	Family with sequence similarity 111, member A	499322	1.79 Up
RSA-14-44	RSA-14-44 protein	297173	1.77 Up
Kif11	Kinesin family member 11	171304	1.70 Up
Vdac1	Voltage-dependent anion channel 1	83529	1.70 Up
Hmgn3	High mobility group nucleosomal binding domain 3	113990	1.69 Up
Nalcn	Sodium leak channel, non-selective	266760	1.69 Up
Tnfrsf14	Tumor necrosis factor receptor superfamily, member 14	366518	1.67 Up
Pex11a	Peroxisomal biogenesis factor 11 α	85249	1.61 Up
RGD1564664	Similar to LOC387763 protein	499839	1.61 Up
LOC100911604	CD99 antigen-like protein 2-like, similar to MIC2L1	500410	-1.14 Down

Table IV. Continued.

C, Exclusively expressed genes in Ma group

Gene symbol	Description	Gene ID	Fold-change
Serpinb1b	Serine (or cysteine) peptidase inhibitor, clade B member 1b, leukocyte elastase inhibitor A-like	306891	-1.15 Down
Mgll	Monoglyceride lipase	29254	-1.15 Down
Lrtomt	Leucine rich transmembrane and 0-methyltransferase domain containing	308868	-1.16 Down
Tas2r145	Taste receptor, type 2, member 145	100363053	-1.18 Down
Kcnip3	Kv channel interacting protein 3, calsenilin	65199	-1.19 Down
Fbll1	Fibrillarin-like 1	363563	-1.19 Down
LOC100910054	NF-κ-B-repressing factor-like	100910054	-1.20 Down
Ttll1	Tubulin tyrosine ligase-like family, member 1	362969	-1.21 Down
Negr1	Neuronal growth regulator 1	59318	-1.22 Down
Ttll11	Tubulin tyrosine ligase-like family, member 11	689746	-1.24 Down
Mgam	Maltase-glucoamylase	312272	-1.25 Down
Apba1	Amyloid β(A4) precursor protein-binding, family A, member 1	83589	-1.26 Down
Hoxb5	Homeo box B5	497987	-1.26 Down
Zfp238	Zinc finger protein 238	64619	-1.27 Down
Ddx6	DEAD (Asp-Glu-Ala-Asp) box helicase 6	500988	-1.29 Down
LOC310902	Similar to Alcohol dehydrogenase 1A (alcohol dehydrogenase αsubunit)	310902	-1.30 Down
Fgf13	Fibroblast growth factor 13	84488	-1.32 Down
Tnnc2	Troponin C type 2 (fast)	296369	-1.33 Down
Pdyn	Prodynorphin	29190	-1.43 Down

log2 (Ratio) Mo, morphine (morphine infusion/vehicle injection/morphine challenge); Up, upregulated; Down, downregulated.

fold change in upregulation; and myocilin has been reported to mediate myelination in the peripheral nervous system (26). Furthermore, microtubule-associated protein 9 expression was decreased in the MOMa group, and this gene has been reported to serve a role in mitotic spindle formation and mitosis progression (27), implying the potential involvement of melatonin.

Reversed gene expression panel between MO/C and MOMa/C groups. In order to clarify which genes were altered by melatonin treatment in morphine-tolerant rats, genes from the microarray data with inverted gene expression profiles between MO/C and MOMa/C groups were selected. Hierarchical clustering analysis was performed to construct a reversed gene expression heatmap between the MO/C and MOMa/C groups (Fig. 3). Genes were selected from the microarray data with the criteria of $\log_2$ ratio ≥1 or ≤-1 and $P<0.05$, and the expression of the genes was reversed between the MO/C and MOMa/C groups. The constructed panel according to the heatmap of the reversed genes was listed in Table V. The panel with inverted gene expression may be used to investigate potential pathways derived by melatonin treatment.

PANTHER pathway mapping and RT-qPCR analysis. The genes listed in Table V-A and -B were used for enrichment analysis by the PANTHER algorithm provided by the GO Consortium. The PANTHER pathway mapped 4 out of 29 genes for the genes listed in Table V-A and 10 out of 66 genes for the genes listed in Table V-B. The PANTHER-mapped pathways and associated genes are listed in Table VI-A and -B. Guanine nucleotide binding protein β polypeptide 1 (Gnb1) was identified to participate in numerous cellular functions, including neuron-associated functions, including glutamatergic, cholinergic, GABAergic, dopaminergic, serotonergic and sympathetic neuron functions. Furthermore, Gnb1 has also been reported to participate in other pathways, including histamine H1 and H2 receptors and several hormone receptor signals. Gnb1 was upregulated 1.4-fold in the MO group and downregulated 1.3-fold in the MOMA group; this result implies the potential of a melatonin-mediated pathway via the repression of G_{β} expression and signaling. On the other hand, the genes mapped in Table VI-B mainly participated in cell proliferation and migration in addition to cytoskeleton reconstruction. For example, a gene named inositol 1,4,5-trisphosphate receptor, type 3 (Itpr3) was downregulated 1.7-fold in the MO group but was upregulated 1.8-fold in the MOMA group. A number of pathways associated with Itpr3, including inflammatory, cell proliferation and migration, G protein mediated and vaso-relaxation pathways, were suggested. The genes mentioned in Table VI-A and VI-B were selected and their

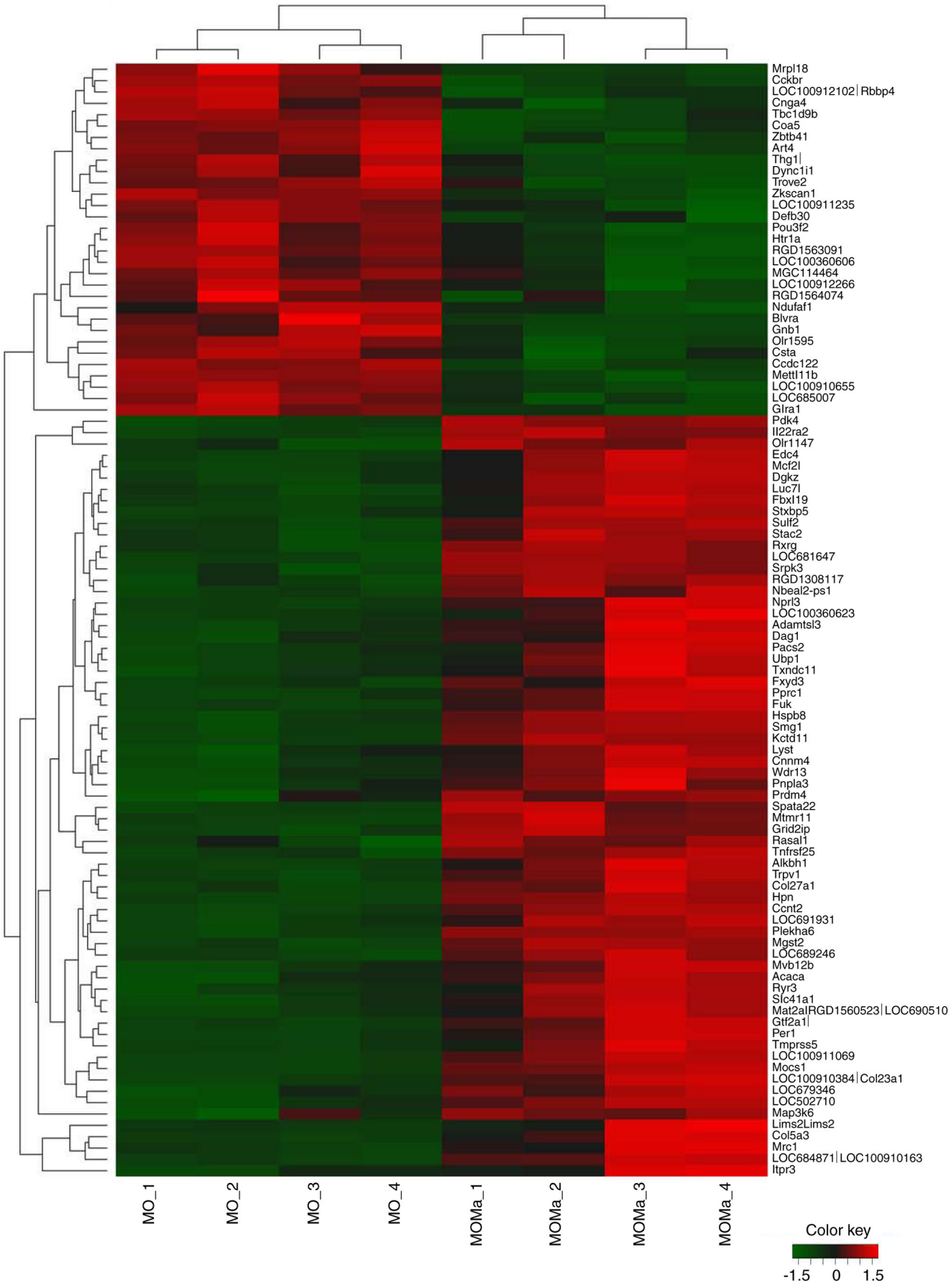

Figure 3. Hierarchical clustering analysis of genes with expression completely inverted between the MO and MOMa group. Upregulated genes are indicated in red, and downregulated genes are presented in green. The signal intensity values of each sample were transformed to $\log_2$ values and subjected to hierarchical clustering using standard correlation. MO, morphine (morphine infusion/vehicle injection/morphine challenge); MOMa, (morphine infusion/melatonin injection/morphine challenge).

Table V. Genes with inverted expressions between Mo and MOMa group

A, Genes with upregulated expression in the MO group but downregulated expression in the MOMa group

Gene symbol	Description	Gene ID	Fold MO	Fold MOMA
Glra1	Glycine receptor, α1	25674	2.10	0.65
Olr1595	Olfactory receptor 1595	304990	1.70	0.66
Ndufaf1	NADH dehydrogenase (ubiquinone) complex I, assembly factor 1	296086	1.42	0.72
RGD1563091	Similar to OEF2	500011	1.40	0.79
Gnb1	Guanine nucleotide binding protein (G protein), βpolypeptide 1	24400	1.40	0.76
Ccdc122	Coiled-coil domain containing 122	100360752	1.39	0.61
Csta	Cystatin A (stefin A)	288067	1.35	0.70
Blvra	Biliverdin reductase A	116599	1.33	0.70
MGC114464	Similar to expressed sequence AI836003	500925	1.32	0.75
LOC100910655	Paralemmin-2-like	100910655	1.31	0.64
Dync1i1	Dynein cytoplasmic 1 intermediate chain 1	29564	1.31	0.79
LOC685007	Similar to unc-93 homolog A	685007	1.30	0.68
Cckbr	Cholecystokinin B receptor	25706	1.29	0.78
Art4	ADP-ribosyltransferase 4	312806	1.29	0.72
Zbtb41	Cytochrome C oxidase assembly factor 5	503252	1.28	0.75
Cnga4	Cyclic nucleotide gated channel α4	85258	1.28	0.78
Thg1l	tRNA-histidine guanylyltransferase 1-like (*S. cerevisiae*)	303067	1.26	0.82
Mettl11b	Methyltransferase like 11B	289167	1.25	0.68
LOC100911235	Mediator of RNA polymerase II transcription subunit 7-like	100911235	1.25	0.81
Htr1a	5-hydroxytryptamine (serotonin) receptor 1A, G protein-coupled	24473	1.24	0.75
Pou3f2	POU class 3 homeobox 2	29588	1.24	0.77

B, Genes with downregulated expression in the MO group but upregulated expression in the MOMa group

Gene symbol	Description	Gene ID	Fold MO	Fold MOMA
Itpr3	Inositol 1,4,5-trisphosphate receptor, type 3	25679	0.59	1.82
Mocs1	Molybdenum cofactor synthesis 1	301221	0.69	1.66
Col5a3	Collagen, type V, α3	60379	0.73	1.66
Mrc1	Mannose receptor, C type 1	291327	0.66	1.65
Lims2	LIM and senescent cell antigen like domains 2	361303	0.65	1.63
Gtf2a1l	General transcription factor IIA, 1-like	316711	0.76	1.58
Olr1147	Olfactory receptor 1147	300408	0.60	1.55
Ccnt2	Cyclin T2	304758	0.82	1.51
Map3k6	Mitogen-activated protein kinase kinase kinase 6	313022	0.64	1.45
Tnfrsf25	Tumor necrosis factor receptor superfamily, member 25	500592	0.71	1.43
Slc41a1	Solute carrier family 41, member 1	363985	0.83	1.43
Mvb12b	Multivesicular body subunit 12B	362118	0.80	1.42
Acaca	Acetyl-CoA carboxylase α	60581	0.77	1.38
Ryr3	Ryanodine receptor 3	170546	0.77	1.38
Col27a1	Collagen, type XXVII, α1	298101	0.83	1.36
Rasal1	RAS protein activator like 1 (GAP1 like)	360814	0.72	1.36
Rasal1	RAS protein activator like 1 (GAP1 like)	360814	0.72	1.36
Mat2a	Methionine adenosyltransferase II	690510	0.79	1.29
er1	Period circadian clock 1	287422	0.63	1.25
Dgkz	Diacylglycerol kinase ζ	81821	0.77	1.24

Mo, morphine (morphine infusion/vehicle injection/morphine challenge); MOMa, (morphine infusion/melatonin injection/morphine challenge).

Table VI. PANTHER pathway mapped cellular functions of four selected genes from Table V-A and -B.

A, PANTHER pathway mapped cellular functions of four selected genes from Table V-A

Gene name	Cellular functions	Pathways
Guanine nucleotide binding protein, β polypeptide 1 (Gnb1)	Neuron	
	Pain_Relief_anagelsia	Opioid proopiomelanocortin pathway
	Pain_Relief_anagelsia	Opioid proenkephalin pathway
	Pain_Relief_anagelsia	Enkephalin release
	Pain_Relief_anagelsia	Cortocotropin releasing factor receptor signaling pathway
	Pain_Relief_anagelsia	Opioid prodynorphin pathway
	Glutamertergic	Metabotropic glutamate receptor group II pathway
	Glutamertergic	Heterotrimeric G-protein signaling pathway-rod outer segment phototransduction
	Glutamertergic	Metabotropic glutamate receptor group III pathway
	Cholinergic	Muscarinic acetylcholine receptor 1 and 3 signaling pathway
	Cholinergic	β1 adrenergic receptor signaling pathway
	Cholinergic	Muscarinic acetylcholine receptor 2 and 4 signaling pathway
	GABAergic	GABA-B_receptor_II_signaling
	GABAergic	Endogenous_cannabinoid_signaling
	Dopaminergic	Dopamine receptor mediated signaling pathway
	Serotonergic	5HT2 type receptor mediated signaling pathway
	Serotonergic	5HT4 type receptor mediated signaling pathway
	Depolarization	Nicotine pharmacodynamics pathway
	Sympathetic	β3 adrenergic receptor signaling pathway
	G protein mediated pathway	β2 adrenergic receptor signaling pathway
	Inflammation	
	G protein mediated pathway	Histamine H1 receptor mediated signaling pathway
	G protein mediated pathway	Histamine H2 receptor mediated signaling pathway
	G protein mediated pathway	Heterotrimeric G-protein signaling pathway-Gq a and Go α mediated pathway
	G protein mediated pathway	Thyrotropin-releasing hormone receptor signaling pathway
	Others	
	Signaling pathway	Gonadotropin releasing hormone receptor pathway
	Signaling pathway	PI3 kinase pathway
	Signaling pathway	Wnt signaling pathway
	Angiogenesis	Angiotensin II-stimulated signaling through G proteins and β-arrestin
	Muscle contraction	Oxytocin receptor mediated signaling pathway
	Cell migration	CCKR signaling pathway
Cholecystokinin B receptor (Cckbr)	Cell migration	CCKR signaling pathway
5-hydroxytryptamine (serotonin) receptor 1A	Neuron_Serotonergic	5HT1 type receptor mediated signaling pathway
G protein-coupled (Htr1a)	G protein mediated pathway	Heterotrimeric G-protein signaling pathway-Gi α and Gs α mediated pathway
Dynein cytoplasmic 1 intermediate chain 1 (Dync1i1)	Neuron	Huntington disease

Table VI. Continued.

B, PANTHER pathway mapped cellular functions of four selected genes from Table V-B

Gene name	Cellular functions	Pathways
Inositol 1,4,5-trisphosphate receptor type 3 (Itpr3)	Inflammation and immunity	Inflammation mediated by chemokine and cytokine signaling pathway Histamine H1 receptor mediated signaling pathwayB cell activation
	Cell proliferation and migration	Gonadotropin releasing hormone receptor pathway Wnt signaling pathway Muscarinic acetylcholine receptor 1 and 3 signaling pathway PDGF signaling pathway
	G protein mediated pathway	Angiotensin II-stimulated signaling through G proteins and β-arrestin Heterotrimeric G-protein signaling pathway-Gq α and Go α mediated pathway
	Vaso relaxation	Endothelin signaling pathway
RAS protein activator like 1 (Rasal1)	Cell proliferation and migration	FGF signaling pathway EGF receptor signaling pathway PDGF signaling pathway
General transcription factor subunit 1-like (Gtf2a1l)	Transcription regulation	Transcription regulation by bZIP transcription 2A General transcription regulation
Period circadian protein homolog 1 (Per1)	Biochemical oscillator Cell proliferation and migration	Circadian clock system Gonadotropin releasing hormone receptor pathway
S-adenosylmethionine synthase isoform type-2 (Mat2a)	Enzyme activity	S adenosyl methionine biosynthesis
Diacylglycerol kinase ζ (Dgkz)	Cell proliferation and migration	Gonadotropin releasing hormone receptor pathway
α4 type V collagen (Col5a3)	Cytoskeleton	Integrin signaling pathway
Collagen α-1(XXVII) chain (Col27a1)	Cytoskeleton	Integrin signaling pathway
LIM and senescent cell antigen-like-containing domain protein (Lims2)	Cytoskeleton	Integrin signaling pathway
Mitogen-activated protein kinase kinase kinase 6 (Map3k6)	Cell proliferation and migration	FGF signaling pathway

gene expressions were verified using RT-qPCR (Fig. 4). All the genes selected here demonstrated an accordance with the expression trends of the microarray results. The results indicate the potential signaling pathways of melatonin in the rat spinal cord for the restoration of cell proliferation and migration through cytoskeleton reconstruction.

Discussion

By using microarray analysis of rat spinal cords from different treatment groups, the gene expression alterations in different conditions were identified. Panels of gene expression with upregulation in the MO group but downregulation in the MOMa group and also inverted gene expression profiles between the MO/C and MOMa/C groups were constructed. Among them, a number of notable genes were identified following PANTHER pathway mapping. For example, Gnb1 is one of the three subunits of heterotrimeric guanine nucleotide binding proteins (G proteins), which integrate signals between G protein coupled receptors (GPCR) (28). GPCR signaling is initiated when a ligand-bound receptor activates heterotrimeric G proteins on the inner leaflet of the plasma membrane by catalyzing the exchange of GDP for GTP on G protein α subunit (Gα), causing it to release the Gβγ subunits. The

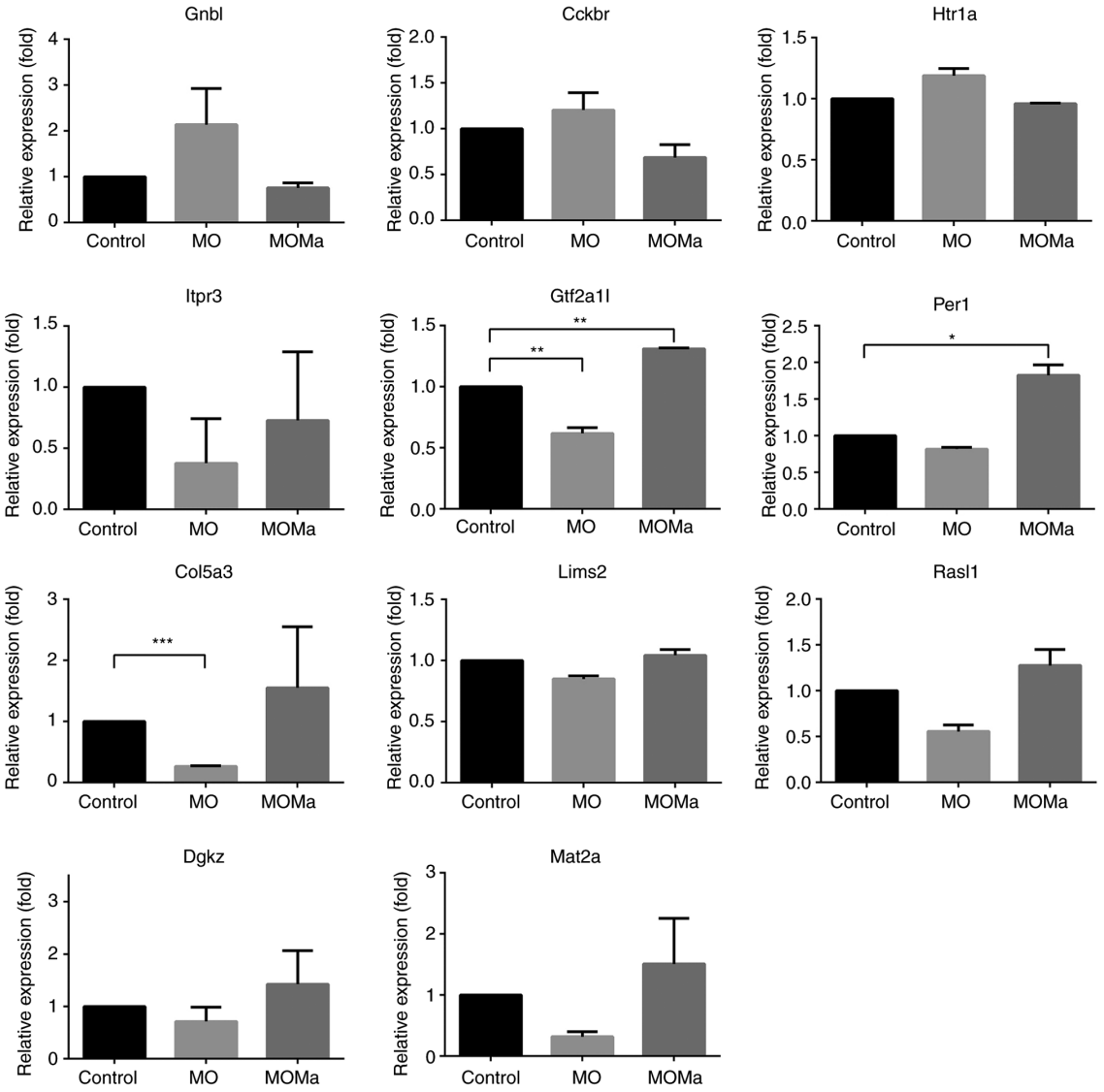

Figure 4. Expressions of genes of interests determined by reverse transcription-quantitative polymerase chain reaction. All expression levels were normalized using GAPDH expression. *P<0.05, **P<0.01 and ***P<0.001 with comparison shown by lines. MO, morphine (morphine infusion/vehicle injection/morphine challenge); MOMa, (morphine infusion/melatonin injection/morphine challenge); Gnb1, guanine nucleotide binding protein β polypeptide 1; Cckbr, cholecystokinin B receptor; Htr1a, 5-hydroxytryptamine receptor 1A; Itpr3, inositol 1,4,5-trisphosphate receptor type 3; Gtf2a1, general transcription factor IIA subunit 1; Per1, period circadian regulator 1; Col5a3, collagen type V α 3 chain; Lims2, LIM zinc finger domain containing 2; RasI1, RAS protein activator like 1, Dgkz, diaglycerol kinase ζ; Mat2a, methionine adenosyltransferase 2A.

GTP-bound Gα and free Gβγ subunits transmit the signal by engaging intracellular effector molecules until GTP is hydrolysed and the β subunits are recoupled to the α subunit to terminate signal transduction receptors and effectors (29). According to a study by Klein *et al* (30), Gnb1 belongs to a group of genes that is night/day differentially expressed in the pineal body; this result implies the potential involvement of Gnb1 in melatonin treatment. Furthermore, β-arrestin-2 mediated desensitization of the μ-opioid receptor is involved in morphine tolerance (31,32). In the present data, Gnb1 was upregulated in the MO group but downregulated by melatonin treatment; this result indicates the potential of a role of melatonin in the activation and desensitization of GPCR.

Another gene, Itpr3, was downregulated in the MO group but upregulated in the MOMA group. It was also produced following PANTHER pathway mapping. Itpr3 is the receptor for inositol 1,4,5-trisphosphate (IP_3), which mediates the release of intracellular calcium (33). Following IP_3 binding, Itpr3 permits calcium flow out of the endoplasmic reticulum (34) and results in the activation of transient receptor potential cation channel subfamily M member 5, which results in membrane depolarization (35). In the case of melatonin treatment with Itpr3 upregulation, it was speculated that depolarization in certain nerve cells in the spinal cord may participate in the melatonin-derived attenuation of antinociceptive morphine tolerance.

In the present model, long-term morphine administration did not affect opioid receptor expression potentially due to the alteration of signal transduction and receptor-G protein coupling. It has been demonstrated that the downregulation of opioid receptors following chronic agonist exposure induces tolerance (36,37). However, a controversial report did not observe the downregulation of opioid receptors in tolerant animals (38). On the other hand, studies suggest that

β-arrestin-2 (Arrb2) binding causes OPR desensitization, and OPR endocytosis and recycling are required for receptor resensitization. This result suggests the potential involvement of Arrb2 with morphine tolerance (31). However, in the present data, the expression of Arrb2 between the groups was similar; the results did not support the potential involvement of Arrb2 with morphine tolerance. Combining the previous discussion with the present data, it was postulated that the expression changes of opioid receptor and Arrb2 are not mandatory for morphine tolerance mechanisms.

There are limitations in descriptive microarray studies. The first limitation is that sequences in the microarray will be refined in newer databases and will result in different outcomes. Secondly, the associations between mRNAs may be different between mice and humans (39). The third limitation is that the gene expression detected by microarrays is descriptive and may not reflect protein expression and subsequent post-transcriptional modifications (40). However, identifying changes in gene expression in tissues with a high-throughput approach remains a good option as it can be performed in one experiment. Even though the present study uses descriptive microarray analysis, a panel of genes that are specifically expressed in morphine-tolerant animals with or without melatonin treatment was produced. As it is impossible to collect the spinal cord from patients, therefore future studies will use drug databases to identify drugs which target the genes of interest in the present study and use the drugs in the same rat models as in the present study to assess the dosage and efficacy of the drug in the treatment of relieving the morphine tolerance. Following that, the drugs with efficacy in the rat model will be used in humans. Next, patients who are under chronic treatment and with morphine tolerance may be recruited to assess the efficacy of the drug in order to ascertain the results of the present and provide novel treatment methods. From the present microarray analysis, novel insight into the molecular profiles associated with morphine tolerance and the effects of melatonin was provided. The present study offers a foundation for future specific hypotheses testing on potential therapeutic targets derived from melatonin treatment in patients with long-term morphine exposure.

Acknowledgements

The authors would like to thank Dr. Chih-Cheng Chien for his advice about the research.

Funding

The present study was supported by research grants from Ministry of Science and Technology (grant no. 105-231 4-B-281-003-MY2) and Cathay General Hospital (grant no. CGH-MR-A10518) in Taiwan.

Authors' contributions

YCC and RYT wrote the manuscript, were responsible for conception and design, data analysis and interpretation. YTS performed the microarray data analysis and interpretation. IJC was in charge of the animal experiments. TYT and YYM performed the RT-qPCR analysis and interpretation. CSW was responsible for conception and design, financial support, administrative support, final approval of manuscript.

Ethics approval and consent to participate

The use of rats in this study adhered to the Guiding Principles in the Care and Use of Animals of the American Physiology Society and was ethically approved by the National Defense Medical Center Animal Care and Use Committee (Taipei, Taiwan).

Patient consent for publication

Not applicable.

Availability of data and materials

The datasets used and/or analyzed during the current study are available from the corresponding author on reasonable request.

Competing interests

The authors declare that they have no competing interests.

References

1. Chen WW, Zhang X and Huang WJ: Pain control by melatonin: Physiological and pharmacological effects. Exp Ther Med 12: 1963-1968, 2016.
2. Pasternak GW: When it comes to opiates, just say NO. J Clin Invest 117: 3185-3187, 2007.
3. Günther T, Dasgupta P, Mann A, Miess E, Kliewer A, Fritzwanker S, Steinborn R and Schulz S: Targeting multiple opioid receptors-improved analgesics with reduced side effects? Br J Pharmacol 175: 2857-2868, 2018.
4. Martini L and Whistler JL: The role of mu opioid receptor desensitization and endocytosis in morphine tolerance and dependence. Curr Opin Neurobiol 17: 556-564, 2007.
5. Rosenblum A, Marsch LA, Joseph H and Portenoy RK: Opioids and the treatment of chronic pain: Controversies, current status, and future directions. Exp Clin Psychopharmacol 16: 405-416, 2008.
6. Pang CS, Tsang SF and Yang JC: Effects of melatonin, morphine and diazepam on formalin-induced nociception in mice. Life Sci 68: 943-951, 2001.
7. Lin SH, Huang YN, Kao JH, Tien LT, Tsai RY and Wong CS: Melatonin reverses morphine tolerance by inhibiting microglia activation and HSP27 expression. Life Sci 152: 38-43, 2016.
8. Song L, Wu C and Zuo Y: Melatonin prevents morphine-induced hyperalgesia and tolerance in rats: Role of protein kinase C and N-methyl-D-aspartate receptors. BMC Anesthesiol 15: 12, 2015.
9. Xin W, Chun W, Ling L and Wei W: Role of melatonin in the prevention of morphine-induced hyperalgesia and spinal glial activation in rats: Protein kinase C pathway involved. Int J Neurosci 122: 154-163, 2012.
10. Feng YM, Jia YF, Su LY, Wang D, Lv L, Xu L and Yao YG: Decreased mitochondrial DNA copy number in the hippocampus and peripheral blood during opiate addiction is mediated by autophagy and can be salvaged by melatonin. Autophagy 9: 1395-1406, 2013.
11. Yahyavi-Firouz-Abadi N, Tahsili-Fahadan P, Riazi K, Ghahremani MH and Dehpour AR: Melatonin enhances the anti-convulsant and proconvulsant effects of morphine in mice: Role for nitric oxide signaling pathway. Epilepsy Res 75: 138-144, 2007.
12. Raghavendra V and Kulkarni SK: Reversal of morphine tolerance and dependence by melatonin: Possible role of central and peripheral benzodiazepine receptors. Brain Res 834: 178-181, 1999.
13. Garmabi B, Vousooghi N, Vosough M, Yoonessi A, Bakhtazad A and Zarrindast MR: Effect of circadian rhythm disturbance on morphine preference and addiction in male rats: Involvement of period genes and dopamine D1 receptor. Neuroscience 322: 104-114, 2016.

14. Fan Y, Liang X, Wang R and Song L: Role of endogenous melatoninergic system in development of hyperalgesia and tolerance induced by chronic morphine administration in rats. Brain Res Bull 135: 105-112, 2017.
15. Chou KY, Tsai RY, Tsai WY, Wu CT, Yeh CC, Cherng CH and Wong CS: Ultra-low dose (+)-naloxone restores the thermal threshold of morphine tolerant rats. J Formos Med Assoc 112: 795-800, 2013.
16. Guiding principles in the care and use of animals of the American physiology society.
17. Grossman ML, Basbaum AI and Fields HL: Afferent and efferent connections of the rat tail flick reflex (a model used to analyze pain control mechanisms). J Comp Neurol 206: 9-16, 1982.
18. Tsai RY, Chou KY, Shen CH, Chien CC, Tsai WY, Huang YN, Tao PL, Lin YS and Wong CS: Resveratrol regulates N-methyl-D-aspartate receptor expression and suppresses neuroinflammation in morphine-tolerant rats. Anesth Analg 115: 944-952, 2012.
19. Pirooznia M, Nagarajan V and Deng Y: GeneVenn-A web application for comparing gene lists using Venn diagrams. Bioinformation 1: 420-422, 2007.
20. Xu J, Kelly R, Fang H and Tong W: ArrayTrack: A free FDA bioinformatics tool to support emerging biomedical research-an update. Hum Genomics 4: 428-434, 2010.
21. Saldanha AJ: Java Treeview-extensible visualization of microarray data. Bioinformatics 20: 3246-3248, 2004.
22. Gene ontology Enrichment analysis website.
23. Mi H, Muruganujan A and Thomas PD: PANTHER in 2013: Modeling the evolution of gene function, and other gene attributes, in the context of phylogenetic trees. Nucleic Acids Res 41 (Database Issue): D377-D386, 2013.
24. Livak KJ and Schmittgen TD: Analysis of relative gene expression data using real-time quantitative PCR and the 2(-Delta Delta C(T)) method. Methods 25: 402-408, 2001.
25. Roeckel LA, Le Coz GM, Gavériaux-Ruff C and Simonin F: Opioid-induced hyperalgesia: Cellular and molecular mechanisms. Neuroscience 338: 160-182, 2016.
26. Kwon HS, Johnson TV, Joe MK, Abu-Asab M, Zhang J, Chan CC and Tomarev SI: Myocilin mediates myelination in the peripheral nervous System through ErbB2/3 signaling. J Biol Chem 288: 26357-26371, 2013.
27. Fontenille L, Rouquier S, Lutfalla G and Giorgi D: Microtubule-associated protein 9 (Map9/Asap) is required for the early steps of zebrafish development. Cell Cycle 13: 1101-1114, 2014.
28. Downes GB and Gautam N: The G protein subunit gene families. Genomics 62: 544-552, 1999.
29. Thal DM, Vuckovic Z, Draper-Joyce CJ, Liang YL, Glukhova A, Christopoulos A and Sexton PM: Recent advances in the determination of G protein-coupled receptor structures. Curr Opin Struct Biol 51: 28-34, 2018.
30. Klein DC, Bailey MJ, Carter DA, Kim JS, Shi Q, Ho AK, Chik CL, Gaildrat P, Morin F, Ganguly S, *et al*: Pineal function: Impact of microarray analysis. Mol Cell Endocrinol 314: 170-183, 2010.
31. Bohn LM, Gainetdinov RR, Lin FT, Lefkowitz RJ and Caron MG: Mu-opioid receptor desensitization by beta-arrestin-2 determines morphine tolerance but not dependence. Nature 408: 720-723, 2000.
32. Zuo Z: The role of opioid receptor internalization and beta-arrestins in the development of opioid tolerance. Anesth Analg 101: 728-734, table of contents, 2005.
33. Nagaleekar VK, Diehl SA, Juncadella I, Charland C, Muthusamy N, Eaton S, Haynes L, Garrett-Sinha LA, Anguita J and Rincón M: IP3 receptor-mediated Ca2+ release in naive CD4 T cells dictates their cytokine program. J Immunol 181: 8315-8322, 2008.
34. Taylor CW and Tovey SC: IP(3) receptors: Toward understanding their activation. Cold Spring Harb Perspect Biol 2: a004010, 2010.
35. Liu D and Liman ER: Intracellular Ca2+ and the phospholipid PIP2 regulate the taste transduction ion channel TRPM5. Proc Natl Acad Sci USA 100: 15160-15165, 2003.
36. Dang VC and Christie MJ: Mechanisms of rapid opioid receptor desensitization, resensitization and tolerance in brain neurons. Br J Pharmacol 165: 1704-1716, 2012.
37. Stafford K, Gomes AB, Shen J and Yoburn BC: mu-Opioid receptor downregulation contributes to opioid tolerance in vivo. Pharmacol Biochem Behav 69: 233-237, 2001.
38. Polastron J, Meunier JC and Jauzac P: Chronic morphine induces tolerance and desensitization of mu-opioid receptor but not down-regulation in rabbit. Eur J Pharmacol 266: 139-146, 1994.
39. Wang L, Liu H, Jiao Y, Wang E, Clark SH, Postlethwaite AE, Gu W and Chen H: Differences between mice and humans in regulation and the molecular network of collagen, type III, alpha-1 at the gene expression level: Obstacles that translational research must overcome. Int J Mol Sci 16: 15031-15056, 2015.
40. Brodsky AN, Caldwell M and Harcum SW: Glycosylation and post-translational modification gene expression analysis by DNA microarrays for cultured mammalian cells. Methods 56: 408-417, 2012.